

 Open access • Journal Article • DOI:10.1063/1.2766856

Mechanisms behind blue, green, and red photoluminescence emissions in CaWO₄ and CaMoO₄ powders — [Source link](#)

[A. B. Campos](#), [Alexandre Zirpoli Simões](#), [Elson Longo](#), [José Arana Varela](#) ...+4 more authors

Published on: 03 Aug 2007 - [Applied Physics Letters](#) (American Institute of Physics)

Topics: [Photoluminescence](#)

Related papers:

- [Spontaneous Raman spectroscopy of tungstate and molybdate crystals for Raman lasers](#)
- [Different origins of green-light photoluminescence emission in structurally ordered and disordered powders of calcium molybdate.](#)
- [Luminescence of CaWO₄, CaMoO₄, and ZnWO₄ scintillating crystals under different excitations](#)
- [Hierarchical Assembly of CaMoO₄ Nano-Octahedrons and Their Photoluminescence Properties](#)
- [Optical absorption of divalent metal tungstates: Correlation between the band-gap energy and the cation ionic radius](#)

Share this paper:    

View more about this paper here: <https://typeset.io/papers/mechanisms-behind-blue-green-and-red-photoluminescence-51lh062cr4>



Mechanisms behind blue, green, and red photoluminescence emissions in CaWO_4 and CaMoO_4 powders

A. B. Campos, A. Z. Simões, E. Longo, J. A. Varela, V. M. Longo, A. T. de Figueiredo, F. S. De Vicente, and A. C. Hernandez

Citation: *Applied Physics Letters* **91**, 051923 (2007); doi: 10.1063/1.2766856

View online: <http://dx.doi.org/10.1063/1.2766856>

View Table of Contents: <http://scitation.aip.org/content/aip/journal/apl/91/5?ver=pdfcov>

Published by the [AIP Publishing](#)



Re-register for Table of Content Alerts

Create a profile.



Sign up today!



Mechanisms behind blue, green, and red photoluminescence emissions in CaWO_4 and CaMoO_4 powders

A. B. Campos, A. Z. Simões, E. Longo, and J. A. Varela
LIEC, IQ, UNESP, P.O. Box 355, Araraquara, 14801-970 São Paulo, Brazil

V. M. Longo^{a)} and A. T. de Figueiredo
LIEC, DEMA e DQ, UFSCar, P.O. Box 676, São Carlos, 13565-905 São Paulo, Brazil

F. S. De Vicente and A. C. Hernandez
IFSC, USP, P.O. Box 369, São Carlos, 13560-970 São Paulo, Brazil

(Received 7 March 2007; accepted 6 July 2007; published online 3 August 2007)

A combined experimental and theoretical study was conducted to analyze the photoluminescence (PL) properties of ordered and disordered CaWO_4 (CW) and CaMoO_4 (CM) powders. Two mechanisms were found to be responsible for photoluminescence emission in CW and CM powders. The first one, in the disordered powders, was caused by oxygen complex vacancies $[\text{MO}_3 \cdot \text{V}_\text{O}^\times]$, $[\text{MO}_3 \cdot \text{V}_\text{O}^\bullet]$ and $[\text{MO}_3 \cdot \text{V}_\text{O}^{\bullet\bullet}]$, where $M = \text{W}$ or Mo , which leads to additional levels in the band gap. The second mechanism, in ordered powders, was caused by an intrinsic slight distortion of the $[\text{WO}_4]$ or $[\text{MoO}_4]$ tetrahedral in the short range. © 2007 American Institute of Physics. [DOI: 10.1063/1.2766856]

Materials belonging to the tungstate and molybdate families have a long history of practical applications and have been the object of extensive research over the past century. The continuous interest in these compounds lies in their excellent optical properties, which form the basis of their wide use as phosphors, laser materials, and scintillation detectors.¹⁻³

In this work, we evaluated the photoluminescence of two distinct CaMoO_4 (CM) and CaWO_4 (CW) powders prepared by the polymeric precursor method, i.e., the crystalline form (structurally ordered) and the other form (structurally disordered) before structural order was reached. We also investigated the electronic structure and optical properties using first-principles calculations based on the density functional theory (DFT). The purpose of employing this synergistic strategy combining experimental results and a theoretical study of the electronic structure was not to explain how photoluminescence (PL) decay occurs, since many valid hypotheses already exist,^{4,5} but to ascertain why it occurs at room temperature in ordered and disordered powders.

Experimental details of the preparation of the powders are described elsewhere.⁶ X-ray diffraction (XRD) patterns were recorded on a (Rigaku-DMax) diffractometer using $\text{Cu K}\alpha$ radiation. Raman spectra were recorded on a RFS/100/S Bruker FT-Raman spectrometer with a Nd doped yttrium aluminium garnet laser providing excitation light at 1064 nm. The PL measurements were taken with a Thermal Jarrel-Ash Monospec 27 monochromator and a Hamamatsu R446 photomultiplier. The 350.7 nm excited wavelength of a krypton ion laser (Coherent Innova) was used, with the nominal output of the laser kept at 200 mW.

Periodic *ab initio* quantum-mechanical calculations based on DFT with the B3LYP hybrid functional were made using the CRYSTAL98 computer code.⁷ The basic sets used for the atomic centers were W,⁷ Mo,⁸ Ca (86-511d3G)⁷ and O (6-31G*).⁷ Four different periodic models were employed:

two primitive cells representing the ordered CM-o and CW-o and two periodic disordered CM-d and CW-d representing the disordered powders. The primitive cell was formed by 12 atoms, where the W and Mo atoms were surrounded by four oxygen atoms in a tetrahedral configuration and the Ca atom was surrounded by eight oxygen atoms in a pseudocubic configuration. Figure 1 depicts the order and disorder models of the CW structure. The CM model is similar so it is not shown here. The disordered primitive cells were created by displacing Mo2 and W2 of 0.3 Å in the direction opposite to an oxygen atom in the vertex.

The XRD pattern of the CM and CW powders annealed at 723, 773, 873, and 973 K for 4 h indicates that both systems were ordered in the long range at all the temperatures investigated. The powders crystallized in a scheelite tetragonal unit cell with a space group $I4_1/a$ in a C_{4h}^6 symmetry.⁹ Rietveld analysis indicated two different interactions in the CW and CM lattices. The first interaction occurred between the O and W atoms in the $[\text{WO}_4]$ cluster and the O and Mo atoms in the $[\text{MoO}_4]$ cluster (short range interaction), while the second one occurred between the $[\text{WO}_4]$ - $[\text{WO}_4]$ clusters in CW and the $[\text{MoO}_4]$ - $[\text{MoO}_4]$ clusters in CM (medium range interaction).

The Raman spectroscopy analysis shown in Fig. 2 indicates that the local point symmetry (short and medium ranges) became progressively ordered in a different kinetics.

The results of the XRD taken at room temperature showed a long-range order or periodicity for CW annealed at 723 K, while the Raman modes were not defined at this tem-

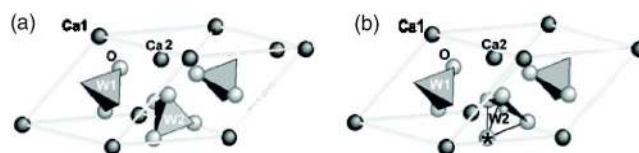


FIG. 1. (Left) CW-o periodic model of the CaWO_4 unit cell. (Right) CW-d periodic model. The W2 was shifted by 0.3 Å in the direction opposite to an oxygen atom O*.

^{a)}Electronic mail: valerialongo@liec.ufscar.br

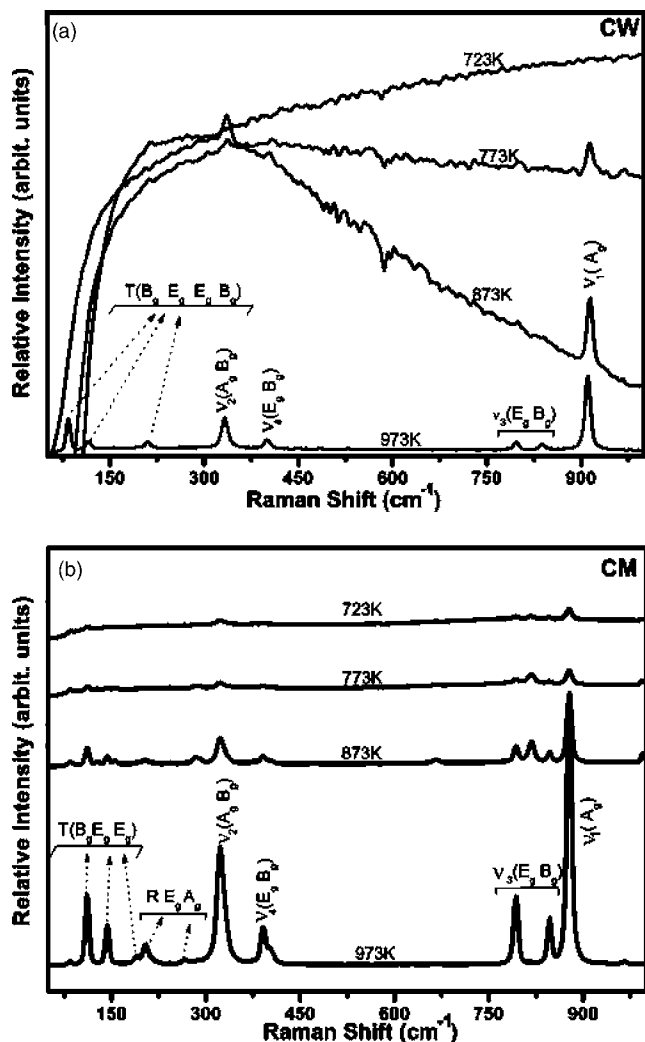


FIG. 2. Room temperature depolarized Raman spectra of powders calcinated at 723, 773, 873, and 973 K for 4 h: (a) CW and (b) CM.

perature [Fig. 2(a)]. This can be explained by the fact that x-ray probes the overall long-range order, whereas Raman scattering probes the short-range structural order. The powder annealed at 873 K showed the O–W–O bending and the W–O₃ torsional modes. Vibrational modes characteristic of scheelite phase in the tetrahedral structure were noted at 973 K. This structure is well organized in the short, medium, and long ranges. Raman spectra of the CM powders showed Raman phonon modes in short-range order at all temperatures investigated [Fig. 2(b)]. The symmetric modes were identified for the tetrahedron group. Hence, the tetrahedron group in the CM structure organizes before the one in the CW tetrahedron group.

According to the *ab initio* calculation,¹⁰ the electron-density contour plots of CW and CM are very similar. These plots show the dominance of the $2p\pi$ states in the upper portion of the valence band and the dominance of the W $5d$ and Mo $4d$ states in the lower portion of the conduction band.

The calculated atom-resolved projected density of states (DOS) area of tungsten, molybdenum, and oxygen in CW-o, CW-d, CM-o, and CM-d models is illustrated in Table I. Only the top of Valence band VB ranging from -5 eV to the Fermi energy was evaluated. The *ab initio* results indicated that the bonding character of the Mo and O in the CM struc-

TABLE I. Gap energy and atom-projected DOS of ordered and disordered CW and CM periodic models. $A_{VB/DOS}$ =area below the VB in total DOS.

$A_{VB/DOS}$	CW-o	CW-d	CM-o	CM-d
W or Mo total	118.0807	103.5297	140.7984	147.2456
O total	1041.4564	984.4048	892.7824	963.7612
% bonding ^a	11.3380	10.5170	15.7707	15.2782
Gap energy	5.27 eV	4.11 eV	5.15 eV	3.98 eV

^a% bonding = $W_{\text{total}} \text{ or } Mo_{\text{total}} / O_{\text{total}}$

ture was stronger than that of the W and O in the CW structure. The disordered CM-d also indicated that a dislocation of 0.3 \AA in the former network slightly modified the bonding character, rendering it different from the CW-d structure. These results indicate that the stronger bonding character organizes the CM lattice during the annealing process, leading to Raman modes even at 723 K.

Figure 3 shows the PL spectra of the CW and CM powders. Numerous papers have discussed the PL behavior of crystalline CW and CM. When excited by short wavelength ultraviolet radiations at room temperature, they present a predominantly blue emission band, which is commonly attributed to the WO₄ tetrahedron.^{11–13} There is also a green emission band, whose origin is still controversial, for it has

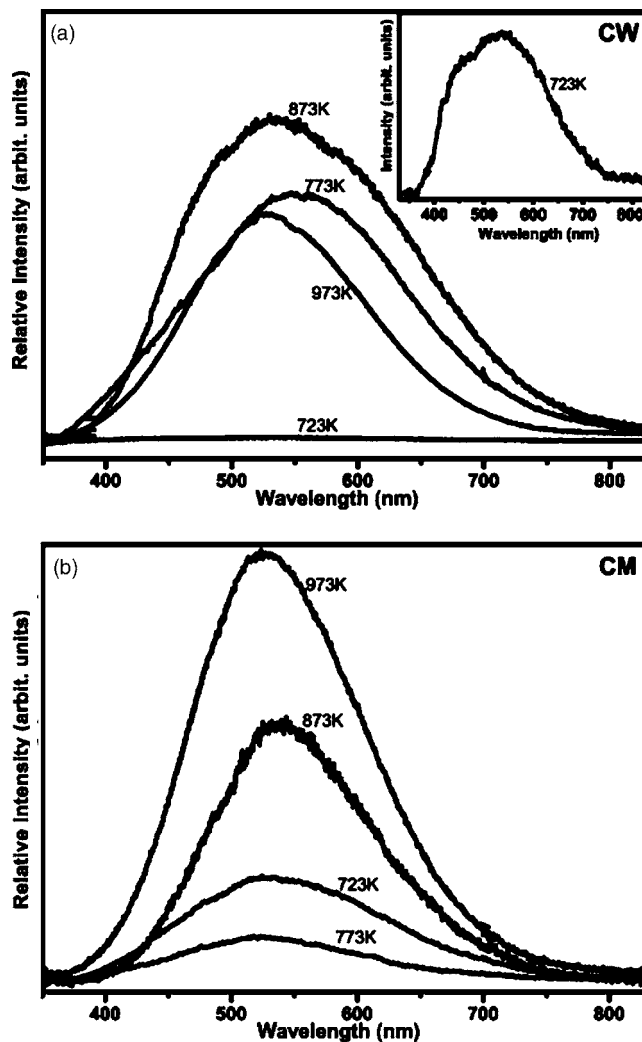


FIG. 3. PL spectrum of powders calcinated at 723, 773, 873, and 973 K for 4 h, excited with the 350.7 nm excited wavelength of a krypton ion laser: (a) CW and (b) CM.

already been attributed to WO_3 defect centers associated with oxygen vacancies¹⁴ as well as to intrinsic transitions in the WO_4^{2-} complex.¹⁵ Lou and Cocivera¹⁵ mention the existence of a red emission band under longer wavelength excitations. According to the literature, $[\text{WO}_3]'$ vacancy-containing complex anions associated with a defect in the sublattice $[\text{WO}_3]'-\text{Ca}^{2+}$ complexes have been identified by the Electron Spin Resonance analysis.¹⁶

Previous results of the PL emission of CW structures recorded with a 488 nm wavelength argon-ion laser indicated broad luminescence behavior in the visible range of the spectra. In this case, its intensity dropped to virtually zero when the crystallization temperature was reached.¹⁷ However, when the 350.7 nm excitation wavelength was used (Fig. 3), the ordered powders remained without emission of the red PL component, although the blue and green PL component increased (450 nm—blue and 550 nm—green) in CW and CM powders. This finding is a strong indication that a more energetic wavelength is able to excite another population of self-trapped electrons present in the well-ordered powders, and that the greenish-blue emission was appropriate for complete periodic order in the medium and long ranges and the disorder in the short range (interaction between W—O or Mo—O). Therefore, we attributed the greenish-blue PL emission to the intrinsic slightly distorted $[\text{WO}_4]$ or $[\text{MoO}_4]$ tetrahedron, according to previous results reported in the literature.^{11–13} In addition, red emission can be associated with the disorder in the long and medium ranges.

In disordered molybdate or tungstate powders, oxygen vacancies can occur in three different charge states: the $[\text{MO}_3 \cdot \text{V}_\text{O}^x]$ state, which captured electrons and was neutral in relation to the lattice, the singly ionized $[\text{MO}_3 \cdot \text{V}_\text{O}^+]$ state, and the doubly positively charged state in the lattice $[\text{MO}_3 \cdot \text{V}_\text{O}^{2+}]$, which did not trap any electrons (where $M = \text{Mo}$ or W). We speculate that these oxygen vacancies induce new energies in the band gap, which can be attributed to molybdenum or tungsten-oxygen vacancy centers. Before donor excitation, a hole in the acceptor and an electron in a donor are created, according to the following equations:



These equations suggest that the oxygen-vacancy-trapped electron in the valence band is a necessary prerequisite

for the transition of a valence-band hole in the conduction band. It must be underscored that this is not a band-to-band transition and that the charge transfer depends on the intrinsic structural defects present in the lattice. As the gap energy increases, so does the structural order (Table I).

In summary, two different mechanisms are responsible for the PL behavior in CW and CM powders at room temperature: disorder caused by $[\text{MoO}_3 \cdot \text{V}_\text{O}^x]$, $[\text{MO}_3 \cdot \text{V}_\text{O}^+]$ and $[\text{MO}_3 \cdot \text{V}_\text{O}^{2+}]$ complex groups in disordered structures and intrinsic slightly distorted $[\text{MoO}_4]$ or $[\text{WO}_4]$ tetrahedral in a short range in the ordered structure. This type of disordered powder is a promising candidate for a wide range of applications in photocatalysis, photochromics, and photoelectric conversion due to its broad optic-response range from violet to red visible light.

The authors thank the financial support of the Brazilian research financing institutions: CAPES, CNPq, and FAPESP.

¹M. Anicete-Santos, F. C. Picon, M. T. Escote, E. R. Leite, P. S. Pizani, J. A. Varela, and E. Longo, *Appl. Phys. Lett.* **88**, 211913 (2006).

²N. Klassen, S. Shmurak, B. Redkin, B. Ille, B. Lebeau, P. Lecoq, and M. Schneegans, *Nucl. Instrum. Methods Phys. Res. A* **486**, 431 (2002).

³F. A. Danevich, A. Sh. Georgadze, V. V. Kobychyev, B. N. Kropyvyansky, V. N. Kuts, A. S. Nikolaiko, V. I. Tretyak, and Yu. Zdesenko, *Phys. Lett. B* **344**, 72 (1995).

⁴R. Leoneli and J. L. Brebner, *Phys. Rev. B* **33**, 8649 (1986).

⁵R. I. Eglitis, E. A. Kotomim, and G. Borstel, *Eur. Phys. J. B* **27**, 483 (2002).

⁶M. A. M. Maurera, A. G. Souza, L. E. B. Soledade, F. M. Pontes, E. Longo, E. R. Leite, and J. A. Varela, *Mater. Lett.* **58**, 727 (2004).

⁷<http://www.crystal.unito.it>

⁸http://www.tcm.phy.cam.ac.uk/~mdt26/basis_set/Mo_basis.txt

⁹Joint Committee on Powder Diffraction Standards (JCPDS) Card No. 41-1431.

¹⁰Y. Zhang, N. A. W. Holzwarth, and R. T. Williams, *Phys. Rev. B* **57**, 12738 (1998).

¹¹V. V. Laguta, J. Rosa, M. I. Zaritskii, M. Nikl, and Y. Usuki, *J. Phys.: Condens. Matter* **10**, 7293 (1998).

¹²M. Martini, F. Meinardi, A. Vedda, M. Nikl, and Y. Usuki, *Phys. Rev. B* **60**, 4653 (1999).

¹³A. A. Blistanov, B. I. Zadneprovskii, M. A. Ivanov, and I. O. Yakimova, *Crystallogr. Rep.* **50**, 284 (2005).

¹⁴B. M. Sinelnikov, E. V. Sokolenko, and E. G. Zvekova, *Inorg. Mater.* **32**, 661 (1996).

¹⁵Z. Lou and M. Cocivera, *Mater. Res. Bull.* **37**, 1573 (2002).

¹⁶V. V. Laguta, M. Martini, A. Vedda, E. Rosetta, M. Nikl, E. Mihokara, J. Rosa, and Y. Usuki, *Phys. Rev. B* **67**, 205102 (2003).

¹⁷E. Orhan, M. Anicete-Santos, M. A. M. A. Maurera, F. M. Pontes, A. G. Souza, J. Andr s, A. Beltr n, J. A. Varela, P. S. Pizani, C. A. Taft, and E. Longo, *J. Solid State Chem.* **178**, 1284 (2005).